（25）FEM Analysis on Interior Beam-Column Joints for Composite EWECS Structural Systems

Kimreth MEAS[1], Hiroshi KURAMOTO[2], FAUZAN[3] and Tomoya MATSUI[4]

[1]Graduate Student, Dept. of Civil Eng., Toyohashi University of Technology
(1-1 Hibarigaoka, Tenpaku cho, Toyohashi, Aichi 441-8580, Japan)
E-mail: meas_kimreth@yahoo.com
[2]Member of JSCE, Associate Professor, Toyohashi University of Technology
(1-1 Hibarigaoka, Tenpaku cho, Toyohashi, Aichi 441-8580, Japan)
E-mail:kura@tutrp.tut.ac.jp
[3]Post-Doctoral Researcher, Dept. of Civil & Arch. Eng., in Toyohashi University of Technology
(1-1 Hibarigaoka, Tenpaku cho, Toyohashi, Aichi 441-8580, Japan)
E-mail:f049101@edu.imc.tut.ac.jp
[4]Assistant Professor, Dept. of Civil & Arch. Eng., in Toyohashi University of Technology
(1-1 Hibarigaoka, Tenpaku cho, Toyohashi, Aichi 441-8580, Japan)
E-mail:matsui@tutrp.tut.ac.jp

This paper presents the results of FEM analytical study on seismic behavior of interior beam-column joints for composite Engineering Wood Encased Concrete-Steel (EWECS) structural systems. The joints consist of EWECS columns and Engineering Wood Encased Steel (EWES) beams. A nonlinear 3-D finite element analysis was used to simulate the seismic behavior of the joints, which is compared with the test data. The analysis took into account the interface interaction between concrete and steel, and that between wood and steel. The main parameter was the types of failure modes; beam flexural failure and joint shear failure. Comparison of analytical and experimental results showed that the analytical prediction for joint shear strength was satisfactory for both types of the joints. In addition, contributions of shear resisting components of steel, concrete and woody shell to the joint shear strength were examined using the proposed numerical model.

Key Words :*EWECS composite structure, beam-column joint, static loading test, FEM analysis*

1. INTRODUCTION

Engineering Wood Encased Concrete-Steel (EWECS) structural system which is a new type of hybrid structural system has been developed by the authors in order to solve a problem for the limitation of story number for wooden structures that is limited to not more than three stories based on the Building Standard Law of Japan. The structure consists of EWECS columns and Engineering Wood Encased Steel (EWES) beams. For the first stage of the research program, EWECS columns using single and double H-section steels had been studied to investigate the seismic performances of the columns[1)-3)]. In the second stage, study on interior beam-column joints for EWECS structural system (EWECS beam-column joints) was carried out to investigate its seismic performance[4)]. This paper summarizes the experimental results and presents analytical study on seismic behavior of EWECS interior beam-column joints subjected to constant axial load and lateral load reversals. A 3-D nonlinear finite element (FEM) analysis was also used to simulate the behavior of the joints, which is compared with the test results.

2. EXPERIMENTAL PROGRAM

(1) Specimen

A total of two interior beam-column joint specimens of about one-third scale were prepared and tested, which simulated the joints for EWECS structural systems. One specimen was designed to fail in beam flexure (WJA) and the other one was designed to fail in joint shear (WJB). The dimensions and details of the specimens are shown in **Fig. 1**. Both specimens had columns with 1,300

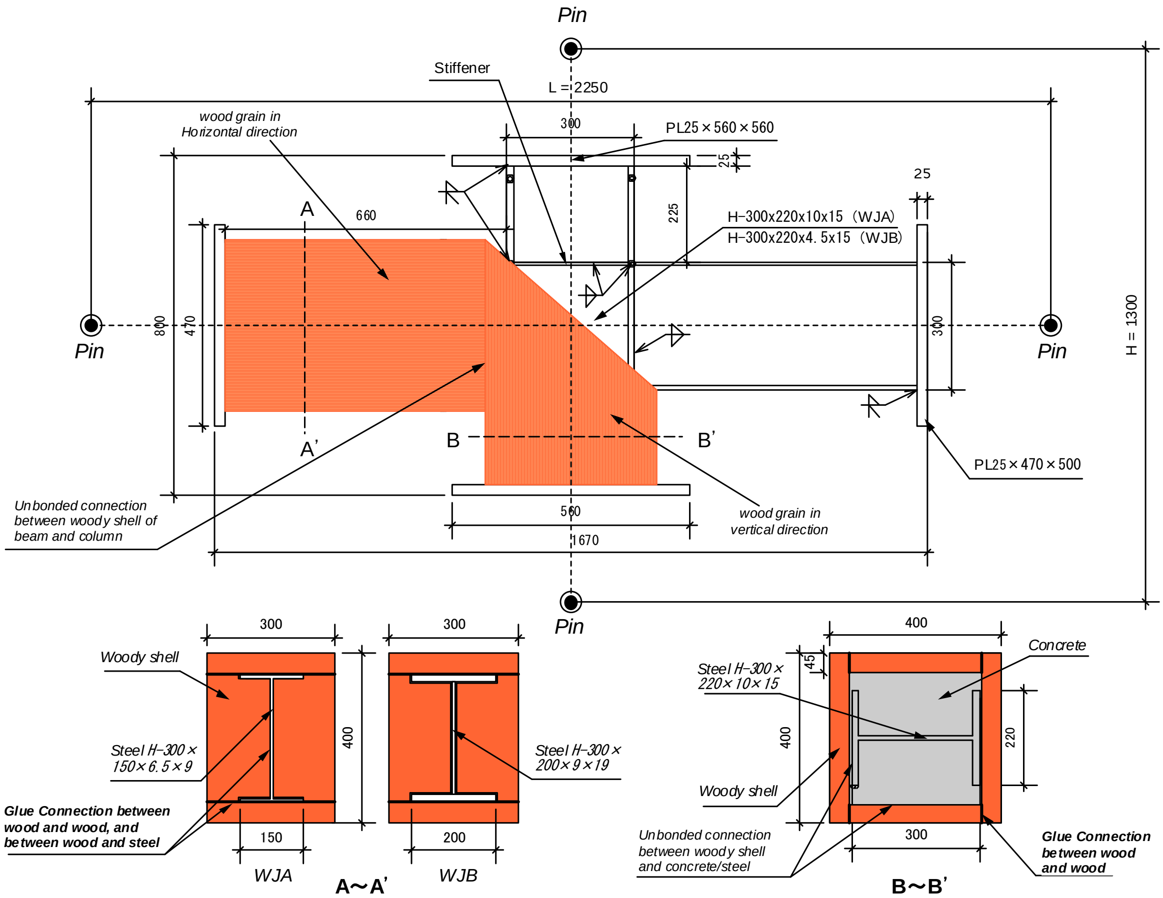

Fig. 1 Test specimen.

mm height and 400mm square section, and beams with 2,250 mm length and 300mm x 400mm section. The steel encased in each column had a single H-section steel of 300x220x10x15 mm and the thickness of the woody shell for the columns was 45 mm. The difference between these two specimens was the encased steel in the beams and joint panels. In both specimens, the woody shell covered the H-section steel of the beams using wood glue.

(2) Test procedure

The specimens were loaded lateral cyclic shear forces by a horizontal hydraulic jack at the top of the column while a constant compression load was applied by two vertical hydraulic jacks. The magnitude of the applied compression load was 615 kN (0.3 N_o; where N_o = total compressive strength of concrete column core).

The incremental loading cycles were controlled by story drift angles, R, defined as the ratio of relatively vertical displacement measured by two vertical transducers installed to a gauge holder at the two ends of the beam, to the distance between the two ends, δ/L. The lateral load sequence consisted of two cycles to each R of 0.005, 0.01, 0.015, 0.02, 0.03 and 0.04 rad. followed by a half cycle to R of 0.05 rad.

2. SUMARY OF THE EXPERIMENTAL RESULT[4)]

(1) Hysteresis characteristics

The story shear versus story drift angle responses of both specimens are given in **Fig. 2**. The yielding and maximum strengths and the corresponding story drift angles for each specimen are listed in **Table 1**.

As shown in **Fig. 2**, both specimens showed a stable shear versus story drift angle response. In Specimen WJA with beam flexural failure, the first yielding occurred on steel flange of the beam when the applied load was 221 kN at R of 0.004 rad. Maximum shear capacity of 435 kN was reached at R of 0.03 rad. The specimen showed stable spindle-shaped hysteresis loops with a little strength degradation after reaching the maximum capacity.

For Specimen WJB with joint shear failure, the first yielding occurred on steel web of the panel zone at shear force of 163 kN and R of 0.0024 rad. The hysteresis curve showed a little pinching-shaped but stable behavior with strength degradation after attaining the maximum capacity of 393 kN at R of 0.015 rad., and retaining more than 75 % of its peak strength at the last story drift R of 0.05 rad. The maximum capacity of this specimen was lower than that of Specimen WJA.

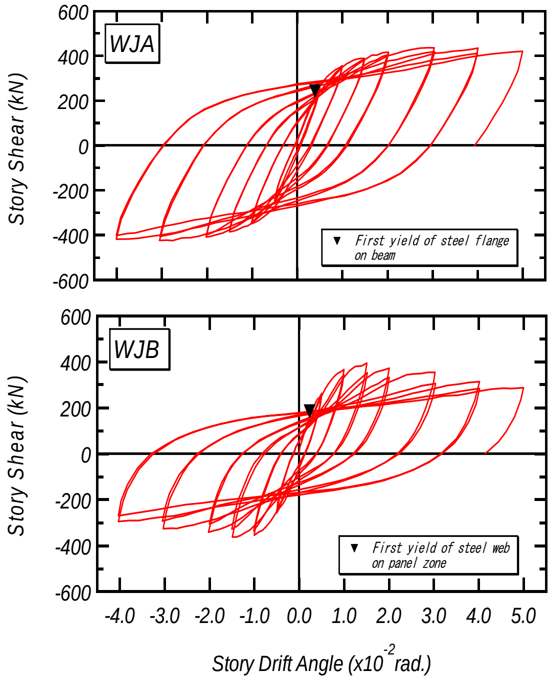

Fig. 2 Story shear - story drift angle relationships.

Table 1 Measured strength

Specimen	at Yielding			at the Max. Capacity	
	Qy (kN)	Ry (rad.)	Location	Qmax (kN)	Rmax (rad.)
WJA	221	0.004	Beam flange	435	0.03
WJB	163	0.0024	Web panel	393.5	0.015

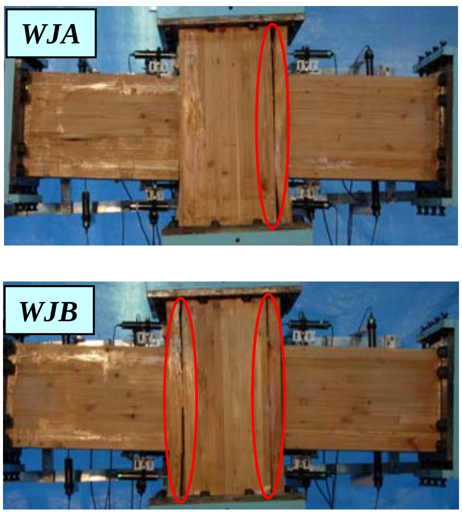

Photo 1 Crack modes of specimens at R of 0.05rad.

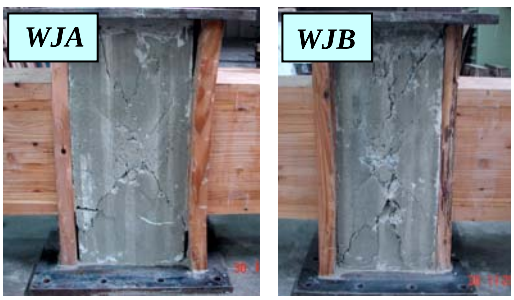

Photo 2 Crack modes of concrete cores after extracting the woody shell.

(2) Failure mode

Different crack patterns were observed for both specimens. Compared to Specimen WJA, more damages of the woody shell on the column faces were observed in Specimen WJB, as shown in **Photo 1**. Up to R of 0.03 rad., a little crack occurred on column face for Specimen WJA, while the splitting of woody shell was observed on the top and bottom of the column face for Specimen WJB. In addition, it was observed for both specimens that only slight damage occurred on woody shell of beams due to sink (embedment) and uplift of beam woody shell that occurred at the connection between woody shells of beams and column.

After testing, the woody shell was removed from front side of the columns to visually inspect the damage on the concrete column core of the joint. It was observed that the in-filled concrete in Specimen WJB had more severe crushed compared with Specimen WJA, as shown in **Photo 2**.

(3) Shear versus joint distortion response

Figure 3 shows the story shear versus joint distortion responses of both specimens. In Specimen WJA, the maximum joint distortion (γ_p) was about 0.012 rad. with the story shear of about 415.5 kN, while in Specimen WJB, the maximum joint distortion was about 0.029 rad. with the maximum shear force of 393.5 kN, which is about 13 % lower than that of Specimen WJA. The higher joint distortion in Specimens WJB might be due to the yielding of web panel first at R of 0.002 rad. and led to the failure of panel zone afterward.

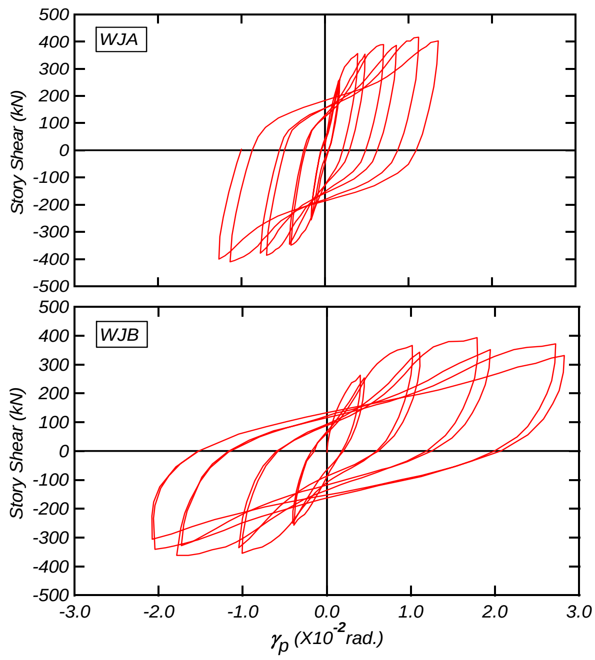

Fig. 3 Joint distortion.

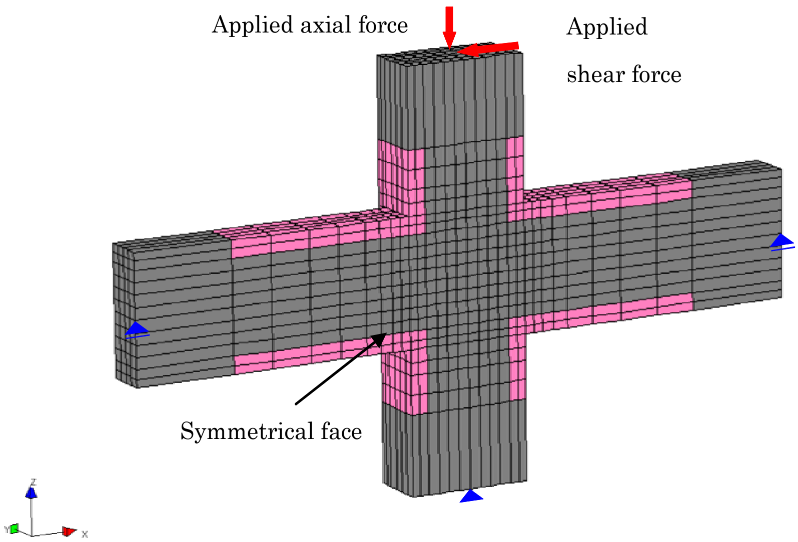

Fig. 4 Finite element idealization.

3. ANALYTICAL MODEL

(1) Finite element modeling of the specimen

In order to compare with the experimental data, FEM analysis of EWECS beam-column joint specimens was carried out by using a nonlinear FEM analysis software package (FINAL version 99) developed by Obayashi Corp[5)]. The specimens were modeled with a total of 4320 elements: 2448 solid elements, 552 of 2-D plane stress elements and 1320 film elements for interface interaction. The structural steel was modeled using 2-D plane stress element and solid element with 8 nodes was modeled for beam and column steel plates. Concrete and wood were also modeled by using solid element. Film element, which took into account the bond-slip effects and crack interface interaction was used to link elements together.

Figure 4 shows the finite element idealization of the specimens. In this figure, half of the specimen was modeled by using the symmetrical condition at the center in longitudinal direction of beam.

(2) Modeling of Concrete

Concrete model took into account cracking and crushing by strain softening while confinement was considered for concrete which bears against the column steel flange. The compressive strength of concrete used in both specimens was 24 MPa. In compression zone, the Saenz equation (Saenz 1964) was used in the ascending zone and a linear decreasing was assumed in the descending zone as shown in **Fig. 5**. The crack is assumed to be initiated perpendicular to the maximum principal stress if its value exceeds the tensile strength, independent of other principal stress. For the basic uniaxial stress-strain relationship, tension softening effect is considered in the tension zone after cracking, as shown in **Fig. 6**.

(3) Modeling of wood

From the result of compressive test in the direction parallel to the annual growth ring of the wood, the peak compressive stress was averagely 45 MPa with corresponding strain of about 0.015 and the modulus of elasticity is 11.59 GPa. Compressive test in the direction perpendicular to the annual growth ring shows that the peak compressive stress is around 5 MPa with corresponding strain of 0.025. In compressive zone bi-linear stress strain relationship is used as shown in **Fig. 7**.

In tension zone, wood model also took into account cracking and crushing by assigning strain softening. The tensile strength of wood in the direction parallel to the annual growth ring was around 60 MPa. Due to the uneffective bonded connection between column woody shell and end column steel plate and also between beam woody shell and end beam steel plate, the maximum tensile strength of woody shell used in the analysis was 5 MPa.

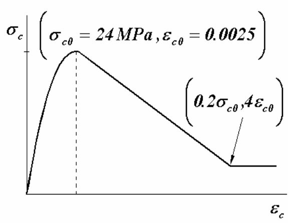

Fig. 5 Stress-strain relationship of concrete in compression.

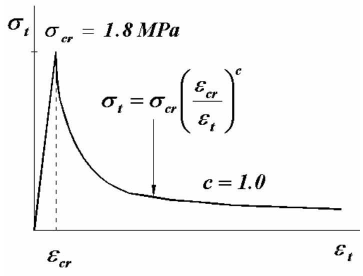

Fig. 6 Stress-strain relationship of concrete in tension.

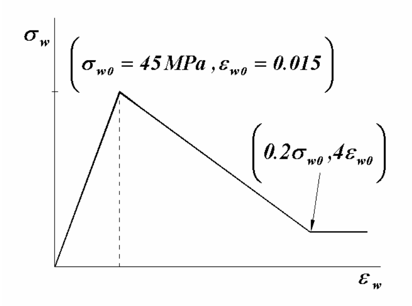

Fig. 7 Stress-strain relationship of wood in compression.

Table 2 Mechanical properties of structural steel.

Steel	Yield Stress (MPa)	Ultimate Stress (MPa)	Specimen	Note
H-300x220	284	450.9	Both	Column Flange
x10x15	295.5	454.9	Specimen	Column Web
PL-10	295.5	454.9	WJAE	Panel Zone
PL-4.5	256.7	337.5	WJBE	Web
H-300x150	320.5	458	WJAE	Beam Flange
x6.5x9	407.7	510.4		Beam Web
H-300x200	251.6	440.8	WJBE	Beam Flange
x9x19	293.1	407.1		Beam Web

(4) Modeling of structural steel

The structural steel was modeled using 2-D plane stress elements. The constitutive behavior of the plate was modeled with von Mises-yield criterion with isotropic strain hardening and an associated flow rule. The mechanical properties of steel is shown in **Table 2**.

(5) Modeling of interaction between concrete and steel

The behavior of the composite structure is highly influenced by the bond-slip effect between concrete and steel, because of the reduction of the composite action caused by relative displacement between these two materials. Kim and Noguchi[6] conducted the experimental study on bond characteristics of concrete and steel plate under monotonic loading. The result of this bond-slip relationship was modified for use in this FEM analysis as the

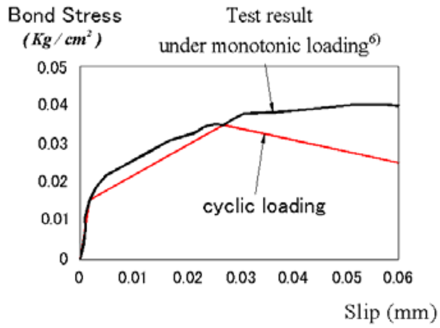

Fig. 8 Bond-slip relationship between concrete and steel.

bond-slip relationship under cyclic loading as shown in **Fig. 8**. In the analysis, film element was used to model this relationship.

(6) Modeling of interaction between wood and steel

Film element was also used to model the bond-slip relationship between the woody shell and the steel of EWES beams. This bond-slip relationship between woody shell and steel was assigned directly in the analysis with much lower stiffness than that of the bond-slip relationship between concrete and steel.

The same bond-slip relationship between woody shell and steel of the beam was used for the bond-slip relationship between the woody shell and the concrete of EWECS column.

(7) Modeling of crack interface interaction

Film element which took into account crack interface interaction was used at the unbonded connection between the column woody shell and the beam woody shell. Only compression was considered in this element to transfer the compressive stress from the beam woody shell to the column woody shell while tension was not considered due to the unbonded surface.

This film element was used to model the crack interaction at the connection between concrete and column end steel plate, and between column woody shell and column end steel plate. In addition, the crack interaction at the connection between beam woody shell and beam end steel plate was also modeled by using this film element.

3. ANALYTICAL RESULT

(1) Shear versus story drift angle responses

The FEM analysis results were compared to the experimental data of EWECS beam-column joint for both types of specimens, as shown in **Fig. 9**. From this figure, it can be seen that the analytical results

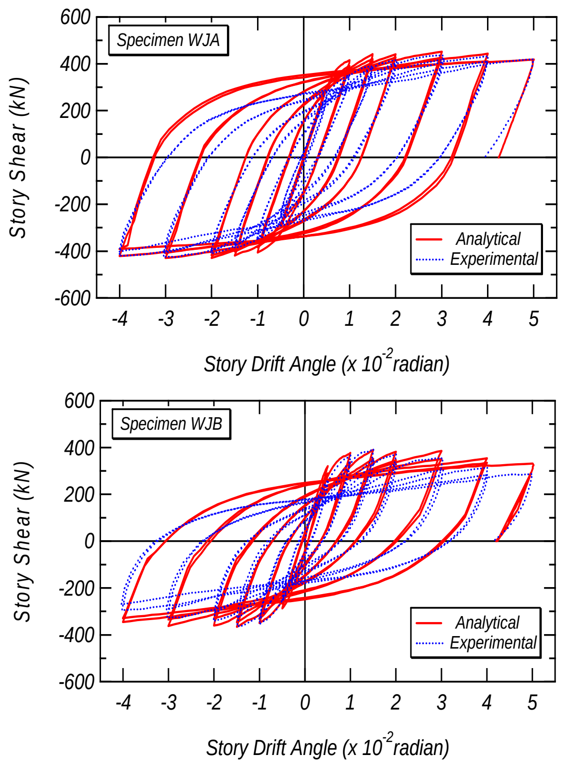

Fig. 9 Story shear –story drift angle relationships.

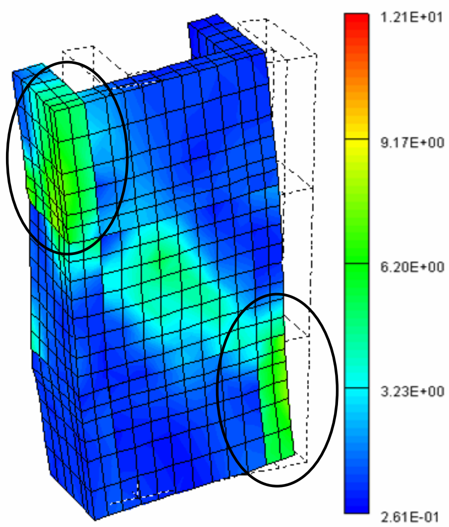

Fig. 10 Minimum shear stress in column woody shell of Specimen WJA.

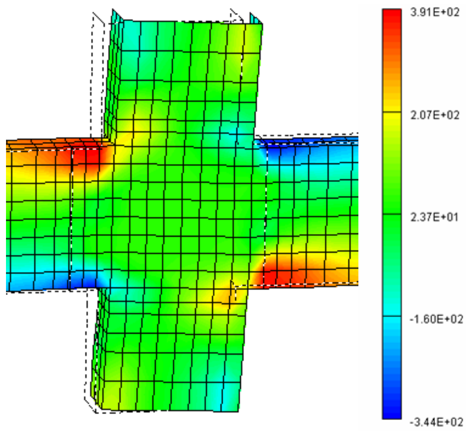

Fig. 11 X-direction axial stress in steel of Specimen WJA.

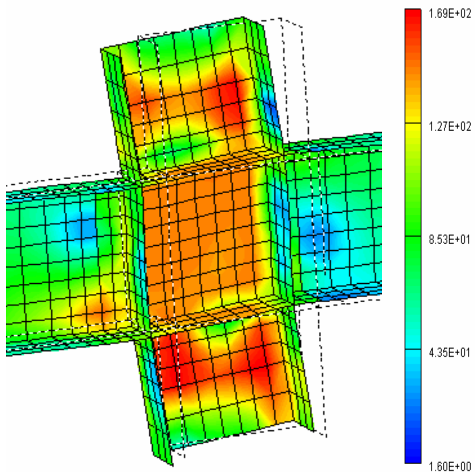

Fig. 12 Maximum shear stress in steel of Specimen WJB.

for shear force versus story drift response of the specimens showed a good agreement with the test results. The analytical models adequately simulated the behavior of the test specimen.

For Specimen WJA, the maximum lateral shear force at story drift angle R of 0.03 rad. from FEM analysis was about only 3% higher than that from experimental one. Until this stage, the prediction of failure mode and the dissipated energy correlates well with the experimental result.

In Specimen WJB, the maximum shear force at R of 0.015 rad. agreed well with the test data while there is a little different pinching shape of the hysteresis loops. The hysteresis loop from FEM analysis also exhibits similar pinching shape and energy dissipation until that story drift angle.

These good comparative results confirmed the accuracy of the proposed numerical analysis to predict the ultimate flexural strength and behavior of EWECS beam-column joints under constant axial load and lateral load reversals.

(2) Principal stress distribution

The result of stress distribution from FEM analysis for both specimens shows that the average nodal stress in concrete compression strut which is mobilized by the column flanges and stiffeners was higher than that in the concrete compression strut which is away from the column flange in the diagonal direction of the panel zone.

The minimum principal stress exceeded the uniaxial compressive strength of concrete in the compression strut region. Moreover maximum principal stress also exceeded the tensile strength of concrete which caused tension-splitting crack formation along the joint panel diagonal.

The panel zone woody shell also contributed its resistance to the joint shear by formation of the compression strut in the diagonal direction of panel zone. The principal stress in that compression strut was still lower than the compressive and tensile strength of the wood for both specimens.

For Specimen WJA, the result of the shear stress distribution in the column woody shell shows that the maximum shear stress from analysis almost exceeds the tangential shear strength of woody shell of around 6 MPa as shown in the circle of **Fig. 10**. It indicates that crack might occur in that location which almost agrees well with the cracking observation from the testing. Then, other cracks propagated along the column height due to the load reversals.

At story drift angle R of 0.03 rad., steel beam flange and web also exhibited significant yielding as shown in **Fig. 11**, while result of the stress distribution shows partial yielding occurred in the panel zone steel. Due to this cracking and yielding, the strength of the specimen decreased after story drift angle R of 0.03 rad. which represented the beam flexural failure.

For Specimen WJB the maximum shear stress in the column woody shell from analysis was higher than that of Specimen WJA and exceeded the tangential shear strength of woody shell due to the significant yielding of the panel zone steel and concrete. This concentration of high shear stress resulted in shear crack to occur in that location. It correlates well with the crack observation during testing, as shown in the circles of Specimen WJB in **Photo 1**. At story drift angle R of 0.015 rad., yielding on column flange and beam flange just started occurring. Panel zone steel exhibits the significant shear yielding, while column web exhibits nearly shear yielding, as shown in **Fig. 12**. This result was agreed well with experimental data.

(3) Shear versus joint distortion responses of Specimen WJB

Figure 13 shows the comparison of the joint distortions of Specimen WJB which was obtained directly from analytical result and the joint distortion obtained from experimental result until story drift angle R of 0.02rad.. In that figure the horizontal axis represents the joint distortion while vertical axis represents the story shear. It indicates that the joint distortion obtained from analytical result was almost similar to the experimental one, but the measured joint distortion exhibited a little more pinching shape than that of analytical result.

(4) Contribution of shear resisting component in the joint

Joint shear force that is difficult to measure from experimental testing can be determined directly from analytical result. The joint shear force is considered to transfer across the mid-plan of the beam column joint in the X-direction. In this analysis, the shear force of each component was calculated by summing up the total of average nodal forces. The joint panel was divided into 3 shear resisting components, concrete, panel zone wood and panel zone steel including column flanges. The ratio of shear resisting components of Specimen WJB from FEM analysis is shown in **Fig. 14.**

The result shows that the contribution of panel zone wood and concrete which is considered as one component is 62% in which the panel zone wood contributed only 14%. In addition, panel zone steel contribution is around 38% from FEM analysis.

4. PARAMETRIC STUDY

To study the contribution of frame mechanism formed by the column steel flanges and stiffeners in the panel zone to the joint shear, the numerical analysis by using the validated finite element model for the interior beam-column joint of Specimen WJB was conducted. In this analysis the story shear versus

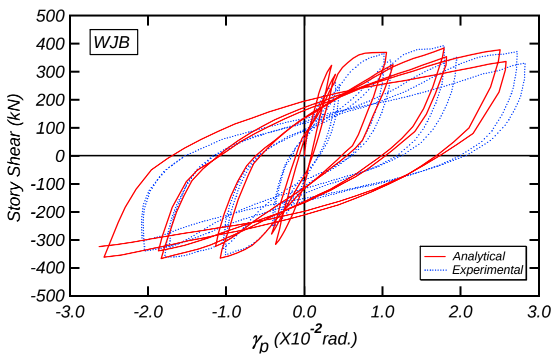

Fig. 13 Comparison of joint distortion.

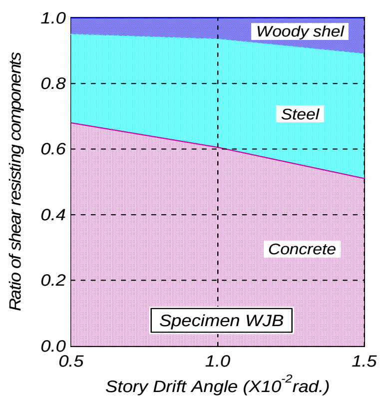

Fig. 14 Ratio of shear resisting component in joint panel of Specimen WJB.

story drift angle response of validated model of Specimen WJB without panel zone steel web was investigated. **Figure 15** shows the comparative result of story shear versus story drift angle responses of validated model of Specimen WJB with and without panel zone steel web.

The result shows that Specimen WJB without panel zone steel web reached it maximum shear capacity of 315 kN at story drift angle R of 0.02 rad. By comparing these two models, the shear capacity for Specimen WJB without panel zone steel was 20% less than the shear capacity of Specimen WJB with steel web. This indicates that the steel web of the panel zone contributed to strength of the joint shear by around 20% of the total joint shear.

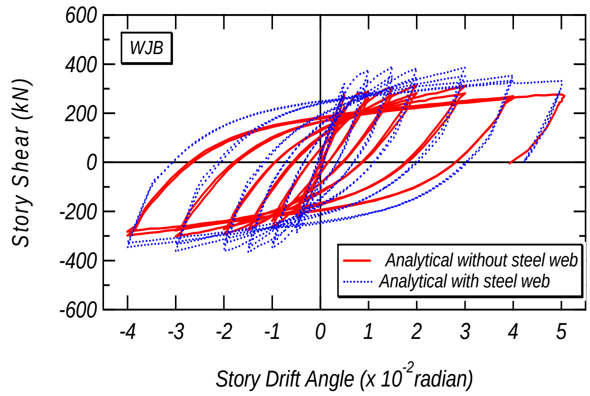

Fig. 15 Story shear versus story drift angle relationship of validated model.

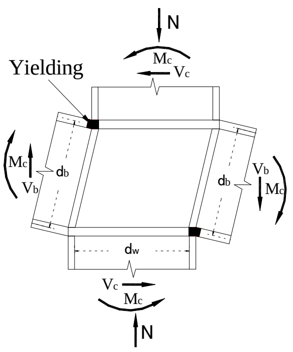

Fig. 16 Frame mechanism.

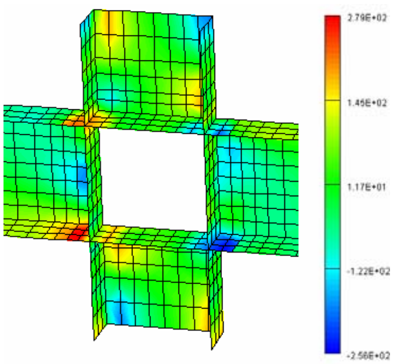

Fig. 17 X-direction axial stress in steel of Specimen WJB in case of no steel web .

From the analytical result of Specimen WJB with steel web of panel zone as mentioned in the section (4), the total panel zone steel contributed to the total joint shear by 38%. Therefore, 18% of the total joint shear was contributed by the steel frame mechanism by the steel flanges and stiffeners in panel zone. This steel frame mechanism was formed by yielding of the beam flange as shown in **Fig. 16**. This yielding is clearly seen from the stress distribution of the result of Specimen WJB without panel, as shown in **Fig. 17**.

5. CONCLUSION

Based on the summary of experimental result and analytical study on the EWECS composite interior beam-column joints by using 3-D nonlinear FEM analysis, the following conclusions can be made:

1. EWECS interior beam-column joints had good structural performance with stable hysteresis behavior.
2. The analytical result using FEM analysis can simulate well the hysteretic behavior of EWECS interior beam-column joint.
3. The FEM analysis result can define the contribution ratio of shear resisting components.
4. Contribution of the frame mechanism in the panel zone by the column flanges and stiffeners to the total joint shear strength was about 18% predicted by using this FEM analysis.

REFERENCES

1) Fauzan, Kuramoto, H. & Ki-Hyung Kim. 2005. Seismic Performance of Composite EWECS Columns Using Single H-Steel, *Proceedings of Japan Concrete Institute*, Vol, 27, No.2, pp. 307-312.
2) Kuramoto, H. & Fauzan. 2005. Feasibility Study on Engineering Wood Encased Concrete-Steel Composite Columns, *Proceedings of 11th ICSGE*, Ain Shams University, Cairo, Egypt, CD-ROM Paper Code-F05ST20.
3) Fauzan, Kuramoto, H., Matsui, T. & Kim, K-H. 2006. Seismic Behavior of Composite EWECS Columns with Varying Shear-Span Ratios, *Proceedings of Japan Concrete Institute*, Vol, 28, No.2, pp. 1357-1362.
4) Fauzan, Kuramoto, H. & Matsui, T. : Seismic Behavior of Interior Beam-Column Joints for Composite EWECS structural systems, Journal of Structural Engineering, Vol. 53B, April 2007.
5) Obayashi Corp., Japan. 2004. Manual of FE analysis package FINAL version 99. Tokyo-Japan.
6) Kim, K., and Noguchi, H. 1994. Experimental Study on bond characteristics of concrete and steel plates. Summary of Technical Papers of Annual Meeting, Architectural Institute of Japan, Tokai, C-1, 163-162. (In Japanese)